

## Collective fluorescence and decoherence of a few nearly identical quantum dots

Anna Sitek and Paweł Machnikowski  
Institute of Physics, Wroclaw University of Technology, 50-370 Wroclaw, Poland

We study the collective interaction of excitons in closely spaced arrays of nearly identical quantum dots with the electromagnetic modes. We discuss how collective fluorescence builds up in the presence of small differences of the transition energy. We analyze also the stability of sub-decoherent states for non-ideally identical systems.

Spatial confinement of carriers in semiconductor quantum dots (QDs) leads to spectrally isolated states which may be optically controlled at a high level of coherence<sup>1</sup>. A single quantum dot offers at most two degrees of freedom (a biexciton) which may be coherently manipulated by optical fields in various ways<sup>2</sup>, allowing one to demonstrate the simplest non-trivial quantum logical operations. In order to go beyond this two-qubit limit towards scalable implementations one needs to develop manufacturing methods and control schemes for arrays of two and more QDs. The optical properties of such quantum dot molecules (QDMs) built of two coupled quantum dots have been experimentally studied for a few years<sup>3</sup>. It has been shown that radiative dephasing of excitons in QDMs differs considerably from that of individual QDs<sup>4</sup>. It was also demonstrated that coupling between neighboring dots may be tuned by external electric field<sup>5</sup>.

Apart from interaction-related effects, resulting from tunnel and dipole coupling between the dots, there is a class of phenomena emerging from collective coupling of many QDs to the electromagnetic (EM) field. These collective effects have been extensively studied for atomic systems<sup>6,7,8,9</sup> where they manifest themselves by superradiant emission, i.e., an outburst of radiation from the excited sample, markedly different from any exponential decay<sup>10</sup>. On the other hand, the collective interaction leads to the appearance of subradiant states for which the probability amplitudes for photon emission interfere destructively, leading to decoupling from the EM reservoir and to infinite lifetime. It has been proposed to use these states for noiseless encoding of quantum information<sup>11</sup> and quantum dot arrays have been suggested as a possible implementation<sup>12</sup>. Compared to atomic samples, quantum dots may be relatively easily arranged in regular arrays but the perfectly identical transition energy characteristic of natural atoms is extremely hard to reach for these artificial systems.

In this Brief Report we study the interaction between small, slightly inhomogeneous arrays of quantum dots and their EM environment. We describe the system evolution within the Weisskopf-Wigner approach<sup>13</sup> and show how the coherent interaction is destroyed by growing inhomogeneity of the transition energies. As important examples, we discuss the buildup of superradiant emission from a few QDs and the decay of "subdecoherent" states built on non-identical QDs. We show also that interaction between dots in a regular array may to some extent stabilize the coherence, in contrast to randomly

distributed atomic systems, where it leads to dephasing<sup>7</sup>.

We consider an array of QDs located at points  $r_j$ . We assume that each dot may either be empty or contain one ground state exciton of fixed polarization with an interband transition energy  $E_j$ , hence can be described as a two-level system. The dots interact with transverse EM modes with frequencies  $\omega_k = ck$ , where  $k$  is the wavenumber and  $c$  is the speed of light. We will describe the system in the interaction picture with respect to the Hamiltonian  $H_0 = E_j \hat{n}_j + \omega_k b_k^{\dagger} b_k$ , ( $\sim = 1$ ), where  $b_k$ ,  $b_k^{\dagger}$  are photon creation and annihilation operators (labels polarizations),  $E$  is the average of the energies  $E_j$  and  $\hat{n}_j$  is the occupation operator for the  $j$ th dot,  $\hat{n}_j = \hat{a}_x^{(j)} \hat{a}_x^{(j) \dagger}$ , where  $\hat{a}_x^{(j)} = \hat{a}_x^{(j)} \hat{a}_y^{(j) \dagger}$  and  $\hat{a}_x \hat{a}_y$  are Pauli matrices acting on the  $j$ th two-level system. The Hamiltonian of the system is  $H = H_X + H_I$ . The first component describes the excitons,

$$H_X = \sum_j \hat{n}_j + \sum_{j \neq j'} V_{1j} \hat{a}_x^{(1)} \hat{a}_x^{(j)}; \quad (1)$$

where  $\epsilon_j = E_j - E$  are the energy deviations from the average and  $V_{1j}$  are Forster couplings between the QDs,

$$V_{1j} = \frac{1}{4 \pi_0 r_{1j}^3} d^2 \frac{3 \hat{d} \frac{\epsilon_j^2}{\epsilon_j^2}}{r_{1j}^2}; \quad r_{1j} = r_j - r_i$$

For self-assembled dots, typical values for this coupling range from 1 eV for the distance between the dots of order of 100 nm to 1 meV for closely stacked dots separated by 10 nm. For extremely closely spaced dots, the coupling will be dominated by tunnelling, which has the same structure as the Forster term. The second term in the Hamiltonian accounts for the interaction with the electromagnetic modes in the rotating wave approximation (RWA)

$$H_I = \sum_k \left( g_k e^{i(\omega_k - E) t} b_k^{\dagger} b_k + H.c. \right); \quad (2)$$

with  $g_k = i d \hat{e}(k) \frac{1}{\omega_k - (2\pi_0 v)}$ , where  $d$  is the interband dipole moment (for simplicity equal for all dots),  $\hat{e}(k)$  are unit polarization vectors,  $\pi_0$  is the vacuum dielectric constant and  $v$  is the normalization volume for EM modes. The QDs are placed at distances much smaller than the relevant photon wavelength so that the spatial dependence of the EM field may be neglected (the Dicke limit). For wide-gap semiconductors with  $E$

eV, zero-temperature approximation may be used for any reasonable temperature.

We will start our discussion with a system of two QDs. The RWA Hamiltonian conserves the number of excitations (excitons plus photons). Let us first consider the initial subradiant state  $j(0)i = (j_{01i} \ j_{10i})^T = \frac{1}{2}$ , where the two-digit kets denote the occupations of the respective dots. Since there is only one excitation in this state it may, in general, evolve into

$$j(t)i = c_{01}(t)j_{01i} + c_{10}(t)j_{10i} + \sum_k c_{00k}(t)j_{00k};$$

where the last ket denotes the state with no excitons and with one photon in the mode  $(k)$ . The Schrödinger equation leads to the system of equations for the coefficients

$$ic_{01} = c_{01} + V c_{10} + \sum_k g_k c_{00k} e^{i(E - \omega_k)t}; \quad (3a)$$

$$ic_{10} = c_{10} + V c_{01} + \sum_k g_k c_{00k} e^{i(E - \omega_k)t}; \quad (3b)$$

$$ic_{00k} = +g_k (c_{01} + c_{10}) e^{i(E - \omega_k)t}; \quad (3c)$$

where  $V = V_{12}$  and  $\omega_2 = \omega_1$ . Following the standard Weisskopf-Wigner procedure<sup>14</sup> we formally integrate Eq. (3c) and substitute to Eqs. (3a,b), which yields

$$c_{01,10} = \frac{i c_{01} - iV c_{10}}{Z_t} dsR(s) (c_{01}(t-s) + c_{10}(t-s));$$

where  $R(s) = \sum_k g_k^2 e^{i(E - \omega_k)t}$  is the memory function of the photon reservoir. As the latter decays extremely quickly compared to the time scales of the evolution of  $c_{01,10}$  one can perform the usual Markov approximation and neglect the  $s$  dependence under the integral. Using the fact that

$$\text{Re} \int_0^t dsR(s) = \frac{E^3 \omega_0^3}{6 \pi^3 c^3} \frac{1}{2};$$

where  $\omega$  is the spontaneous decay rate (throughout the paper we set  $\omega = 1$  ns), and neglecting the imaginary part (i.e., assuming that the Lamb shift and other radiative corrections are included in the energies) one gets

$$c_{01} = i c_{01} - iV c_{10} - \frac{1}{2} (c_{01} + c_{10}); \quad (4a)$$

$$c_{10} = i c_{10} - iV c_{01} - \frac{1}{2} (c_{01} + c_{10}); \quad (4b)$$

The reduced density matrix for the charge subsystem may now be easily constructed as  $\rho_{01,01} = |c_{01}|^2$ ,  $\rho_{10,10} = |c_{10}|^2$ ,  $\rho_{01,10} = \rho_{10,01} = c_{01} c_{10}^*$ ,  $\rho_{00,00} = 1 - \rho_{01,01} - \rho_{10,10}$ , with all other elements equal to 0.

In order to test the stability of the ideally subradiant state in the case of non-identical dots we denote by

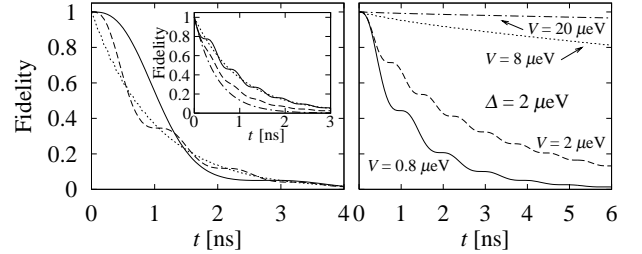


FIG. 1: (a) The fidelity for a subradiant state for  $V = 0$  and  $V = 0.8$  eV (solid), 2 eV (dashed) and 20 eV (dotted). (b) The fidelity for  $V = 0$ ,  $\Delta = 2$  eV. Inset in (a) shows the fidelity of a superradiant state for different dots without interaction ( $E = 4$  eV, solid) and for interacting dots ( $E = 2.68$  eV,  $V = 2.97$  eV, dashed), compared to an exponential decay with the rate 2 (dotted and dash-dotted, respectively).

$j(t)i$  the pure state evolving from  $j(0)i$  in the absence of the EM reservoir ( $E = 0$ ) and define the fidelity of the actual state by  $F = \frac{1}{h(t)} j(t) j(t)i$ . In Fig. 1a we show the result for a few values of the energy difference in the limit of vanishing Forster coupling between the dots (i.e., for sufficiently distant dots). It is clear that the state maintains its subradiant (stable) character until  $t = 2$  ns but then it enters a superradiant phase and the fidelity rapidly decays below the value corresponding to an exponential (uncorrelated) decay. Depending on the value of  $V$ , a certain number of oscillations around this uncorrelated decay rate may be observed. In the limit of large  $V$  these oscillations become very fast, their amplitude decreases, and the decay closely follows that of uncorrelated systems, as expected for systems with large energy difference and therefore interacting with disjoint frequency ranges of the photon reservoir. It is clear that observing collective effects for such non-interacting dots requires transition energies identical up to several eV.

If the QDs are close enough, the Forster interaction becomes effective. Since the sub- and superradiant states are eigenstates of the Forster Hamiltonian separated by an energy  $2V$ , the transition from the initially subradiant state to the superradiant state is suppressed if the magnitude of the Forster coupling exceeds the energy difference  $\Delta$ . This is shown in Fig. 1b. It is clear that the decay rate is reduced when  $V > \Delta$  and the subradiance is recovered for  $V > \Delta$ . Note that, apart from the trivial limiting cases, the decay is markedly non-exponential and its modulation yields information on the origin of the energy level splitting in the system. Indeed, the decay of the superradiant state  $j(0)i = (j_{01i} \ j_{10i})^T = \frac{1}{2}$  shown in the inset to Fig. 1a is clearly different for two systems with the same energy splitting, depending on whether the splitting originates from the difference between the dots or from the interaction.

In the present state of the art of QD manufacturing, the differences between the transition energies of the two dots are rather in the meV than in the eV range. In Fig. 2 we show the evolution for the initial

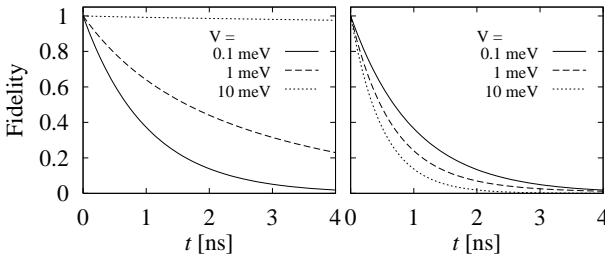


FIG. 2: The fidelity for sub- (a) and superradiant (b) states for  $V = 1 \text{ meV}$ .

states  $j(0)i = (j01i \quad j10i) = \frac{p}{2}$  for  $V = 1 \text{ meV}$ . In this case the rotation between the subradiant and superradiant states is very fast and the decay of the states is smooth. For  $V = 0$ , both states show simple exponential decay with the rate  $\gamma$ . In the opposite limit,  $V \rightarrow \infty$ , the subradiant state becomes stable while the superradiant state decays exponentially with a twice larger rate. In the intermediate range of parameters, the decay is not exponential.

Next, let us consider the case of the same two QDs, but initially excited to the  $j11i$  state. The general form of the state is now

$$\begin{aligned} j(t)i &= c_{11}(t)j11i \\ &+ c_{01k}(t)j01k_i + c_{10k}(t)j10k_i \\ &+ c_{00k} \sum_{q=0}^k (t)j0;qk_i \\ &+ c_{k;q} \sum_{q=0}^k (t)j1;qk_i; \end{aligned}$$

and the amplitudes evolve according to the equations

$$ic_{11} = g_k (c_{01k} + c_{10k}) e^{i(E - \epsilon_k)t}; \quad (5a)$$

$$\begin{aligned} ic_{01k} &= c_{01} + V c_{10} + g_k c_{11} e^{i(E - \epsilon_k)t} \\ &+ g_q c_{00k} e^{i(E - \epsilon_q)t}; \end{aligned} \quad (5b)$$

$$\begin{aligned} ic_{10k} &= c_{10} + V c_{01} + g_k c_{11} e^{i(E - \epsilon_k)t} \\ &+ g_q c_{00k} e^{i(E - \epsilon_q)t}; \end{aligned} \quad (5c)$$

$$ic_{00k} = g_q (c_{01k} + c_{10k}) e^{i(E - \epsilon_q)t}; \quad (5d)$$

As previously, we formally integrate Eq. (5d), insert it into Eqs. (5b,5c), and use the short memory assumption. This yields the equation for  $c_k = (c_{10k}; c_{01k})^T$ ,

$$c_k = ig \int_0^t ds e^{\hat{A}(t-s)} c_{11}(s) e^{i(E - \epsilon_k)s} b; \quad (6)$$

where  $b = (1;1)^T$  and

$$\hat{A} = \begin{pmatrix} i & =2 & iV & =2 \\ iV & =2 & i & =2 \end{pmatrix}.$$

Substituting this in turn into Eq. (5a) we find

$$c_{11} = \int_0^t ds R(s) b^T e^{\hat{A}^* s} b c_{11}(t-s);$$

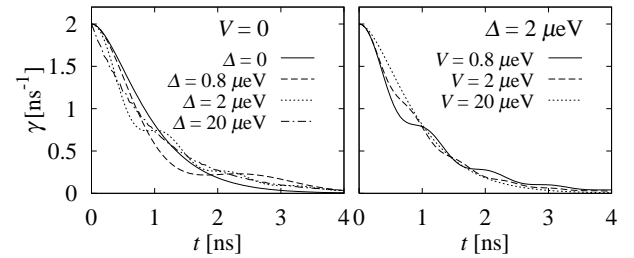


FIG. 3: Photon emission rate for a superradiant state for  $V = 0$  (a) and for  $V \in 0, 2 \text{ eV}$ .

Since the elements of  $\hat{A}$  are of order of  $\text{eV or meV}$ , the matrix exponent is slowly varying on the time scales of reservoir memory, as is  $c_{11}(t)$ , and both may be taken at  $s = 0$ , which leads to the decay equation in the usual form  $c_{11} = -\gamma c_{11}$  or, for the corresponding element of the reduced density matrix,  $\gamma_{11,11} = -2 \gamma_{11,11}$ .

The evolution equations for the other elements of the density matrix may be found by writing, for instance,  $\dot{c}_{01,01} = 2 \text{Re } \epsilon_k (c_{10k} \bar{c}_{01k})$ , substituting  $c_{10k}$  from Eq. (6), and using once more the short memory approximation. Performing this procedure for all the elements of the single-exciton sector, one arrives at the equations

$$\begin{aligned} \dot{f}_{11} &= -2 f_{11}; \\ \dot{f}_{10} &= (\text{Re } p + f_{10} - f_{11}) + 2V \text{Im } p; \\ \dot{f}_{01} &= (\text{Re } p + f_{01} - f_{11}) - 2V \text{Im } p; \\ p &= 2i p \left( p + \frac{f_{01} + f_{10}}{2} - f_{11} \right) \\ &\quad + iV (f_{01} - f_{10}); \end{aligned}$$

where we denoted  $f_{1j} = c_{1j} \bar{c}_{1j}$ ,  $j = 0, 1$ , and  $p = c_{01,10}$ .

The photon emission rate  $\gamma = (f_{11} + f_{01} + f_{10})$  for the initial state  $j11i$  is plotted in Fig. 3. In the case of  $V = 0$  (Fig. 3a) we see that the photon emission loses its superradiant behavior for growing energy difference between the dots, tending to the usual exponential decay for large  $\Delta$ . Similarly as in the previous case, removing the degeneracy between the sub- and superradiant single-exciton states by including the Forster coupling stabilizes the collective fluorescence (Fig. 3b).

In general, the Weisskopff-Weingarten equations lead to the Lindblad equation for the evolution of the reduced density matrix of the charge subsystem

$$\dot{\rho} = -i[H_X, \rho] + L[\rho]; \quad (7)$$

with  $L[\rho] = \sum_j [ \rho + (1/2) f_{1j} + f_{0j}; g_{+} ]$ , where  $\rho = \rho_{(j)}$ .

We now use Eq. (7) to study the evolution of four QDs forming a square array in the  $xy$  plane. The energy deviations of individual dots are now  $\epsilon_1 = \epsilon_2 = \epsilon_3 = \epsilon_4$ , where we arbitrarily  $\epsilon_1 = 0$ ,  $\epsilon_2 = 0.8$ ,  $\epsilon_3 = 0.27$ ,  $\epsilon_4 = 0.54$  and use the mean square variation  $\sigma^2$  as a parameter. The Forster interaction is parameterized by its magnitude  $V$ , with  $V_{12} = V_{23} = V_{34} = V_{41} = V$  and  $V_{13} = V_{24} = 2^{3/2}V$  (the dots are numbered clockwise).

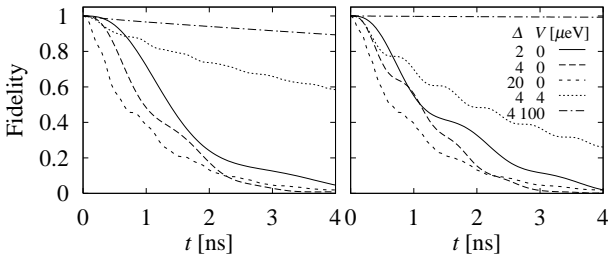


FIG. 4: The fidelity for two subradiant states  $j_{a1}$  (a) and  $j_{b1}$  (b) of 4 QDs for various combinations of parameters. The parameter values given in (b) are valid for both figures.

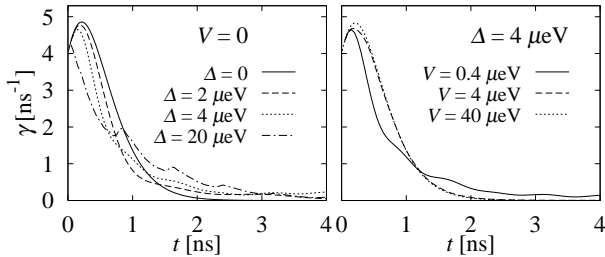


FIG. 5: Photon emission rate for a superradiant state of 4 QDs for  $V_{ij} = 0$  (a) and for  $V_{ij} \neq 0$  (b).

First, let us choose the subradiant initial states  $j_{a1}(0)i = (j_{1001i} - j_{1011i} - j_{1101i} - j_{1010i})/2$  and  $j_{b1}(0)i = (j_{1001i} + j_{0111i} + j_{1101i} - j_{1100i})/2$ , which span the subspace of logical qubit states that may be used for noiseless encoding of quantum information on four physical qubits<sup>11</sup>. Obviously, for non-identical dots the phases in these superpositions will rotate and the state will be driven out of the initial noiseless subspace

which leads to a decrease of fidelity, as shown in Fig. 4. Out of the two states, only  $j_{b1}(0)i$  is a non-degenerate eigenstate of the Frohlich interaction for the square array. As a result, as can be seen in Fig. 4, only this state is fully stabilized by the Forster interaction for  $V = 100$   $\mu$ eV (the lines for  $V = 100$   $\mu$ eV in Fig. 4 are very close to the asymptotic case of  $V \gg 1$ ). This stabilization results from the special, regular arrangement of the QDs and should be contrasted with the dephasing induced by analogous interactions in the randomly distributed atomic samples<sup>7</sup>. Since the other state  $j_{a1}(0)i$  is never completely stable the entire "noiseless subspace" of logical states<sup>12</sup> remains stable only for an extremely homogeneous array of QDs.

Finally, let us study the phonon emission rate from a superradiant state of four excited QDs,  $j_{1111i} = j_{11111i} - j_{11110i} - j_{11101i} - j_{11100i} = 2$  (Fig. 5). Now, a clear superradiant peak of photon emission develops for identical dots but vanishes as the dots become different. Again, interaction between the dots in a regular array stabilizes the collective emission. It is interesting to note that the superradiant emission is close to ideal already for  $V = 100$   $\mu$ eV, while the subradiant states are stabilized only when the interaction exceeds the energy difference by an order of magnitude.

We have shown that collective interaction of carriers in QDs with their EM environment is extremely sensitive to the homogeneity of the QD array. The destructive effect of inhomogeneity can be to some extent overcome by excitation-transfer coupling (Forster or tunneling) between the dots placed in a regular array. This can stabilize the subradiance of a state of 2 QDs and the superradiant emission from 4 QDs but (for a square alignment) cannot stabilize the entire noiseless subspace of 4 QDs.

Electronic address: Paweł Machnikowski@pwrwroc.pl

<sup>1</sup> A. Zrenner, E. Beham, S. Stuer, F. Fiedeis, M. Bichler, and G. Abstreiter, *Nature* **418**, 612 (2002); S. Stuer, P. Ester, A. Zrenner, and M. Bichler, *Phys. Rev. B* **72**, 121301 (2005).

<sup>2</sup> X. Li, Y. Wu, D. Steel, D. Gammie, T. Stievater, D. Katzer, D. Park, C. Piamirocchi, and L. Sham, *Science* **301**, 809 (2003); S. Stuer, P. Machnikowski, P. Ester, M. Bichler, V. M. Axt, T. Kuhn, and A. Zrenner, *Phys. Rev. B* **73**, 125304 (2006).

<sup>3</sup> M. Bayer, P. Hawrylak, K. Hinxer, S. Fafard, M. Korkusinski, Z. R. Wasilewski, O. Stelm, and A. Forchel, *Science* **291**, 451 (2001); G. Oltner, M. Bayer, A. Larionov, V. Timofeev, A. Forchel, Y. B. Lyanda-Geller, T. L. Raincke, P. Hawrylak, S. Fafard, and Z. R. Wasilewski, *Phys. Rev. Lett.* **90**, 086404 (2003); T. Unold, K. Mueller, C. Lienau, T. Elsaesser, and A. D. Wieck, *Phys. Rev. Lett.* **94**, 137404 (2005).

<sup>4</sup> P. Borsig, W. Langbein, U. Woggon, M. Schwab, M. Bayer,

S. Fafard, Z. R. Wasilewski, and P. Hawrylak, *Phys. Rev. Lett.* **91**, 267401 (2003).

<sup>5</sup> H. J. Krenner, M. Sabathil, E. C. Kark, A. Kress, D. Schuh, M. Bichler, G. Abstreiter, and J. J. Finley, *Phys. Rev. Lett.* **94**, 057402 (2005).

<sup>6</sup> H. M. Nussenzweig, *Introduction to Quantum Optics* (Gordon and Breach, New York, 1973).

<sup>7</sup> M. G. Ross and S. Haroche, *Phys. Rep.* **93**, 301 (1982).

<sup>8</sup> R. H. Dicke, *Phys. Rev.* **93**, 99 (1954).

<sup>9</sup> R. H. Lehmberg, *Phys. Rev. A* **2**, 883 (1970); **2**, 889 (1970).

<sup>10</sup> N. Skribanowitz, I. P. Hermann, J. C. MacGillivray, and M. S. Feld, *Phys. Rev. Lett.* **30**, 309 (1973).

<sup>11</sup> P. Zanardi and M. Rasetti, *Phys. Rev. Lett.* **79**, 3306 (1997).

<sup>12</sup> P. Zanardi and F. Rossi, *Phys. Rev. Lett.* **81**, 4752 (1998).

<sup>13</sup> V. W. Weisskopf and E. Wigner, *Z. Phys.* **63**, 54 (1930).

<sup>14</sup> M. O. Scully and M. S. Zubairy, *Quantum Optics* (Cambridge University Press, Cambridge, 1997).